Proceedings of FEDSM '03
4TH ASME_JSME Joint Fluids Engineering Conference
Honolulu, Hawaii, USA, July 6-11, 2003

FEDSM2003-45067

BULK CARBON NANOTUBES FOR MICRO ANEMOMETRY

Victor T.S. Wong and Wen J. Li
Centre for Micro and Nano Systems
The Chinese University of Hong Kong
Hong Kong SAR

ABSTRACT

We have successfully developed a process to manipulate post-growth multi-walled carbon nanotube (MWNT) by AC electrophoresis to form resistive elements and showed that these elements can potentially served as novel sensing elements for micro/nano thermal and anemometry sensing. We have measured the temperature coefficient of resistance (TCR) of these MWNT bundles and integrated them into constant current mode configuration for dynamic characterization. Preliminary experimental measurements showed that the devices could be operated in micro-watt power range for micro thermal and anemometry sensing. This operation range is three orders of magnitude lower than conventional Micro-Electro-Mechanical Systems (MEMS) polysilicon sensors in constant current (CC) mode configuration. In addition, the devices exhibited very fast frequency response (> 100 kHz) in CC mode. Based on these results, we are currently developing polymer-based MWNT embedded sensor for various micro/nano fluidic applications.

Keywords: Carbon nanotube (CNT), AC electrophoresis, Micro anemometry, Micro/Nano resolution sensor, Polymer-based MWNT embedded sensor.

INTRODUCTION

Power consumption is one of the most important considerations in designing electronic circuit and MEMS devices. since high power consumption implies high heat dissipation which is undesirable in many applications. A typical example is the wall shear stress measurement in aerodynamic applications using integrated MEMS sensors [1]. Excessive heat dissipation from a hot film anemometrical sensor will disturb the minute fluidic motion, crippling the ability to sense true fluidic parameters. Therefore, in order to detect the fluidic parameters in a finer resolution, sensing elements with low power consumption are necessary. From our experimental measurements, we found that MWNT bundles consumed only μW power during thermal sensing operation (compared with mW for MEMS polysilicon sensor). In other words, using MWNT bundles for fluidic sensing will significantly reduce the thermal disturbance to the flow parameters to be measured when compared with MEMS polysilicon sensors.

In order to incorporated MWNT bundles as sensing elements, techniques to manipulate MNWT has to be developed. Typical active manipulation technique is by atomic force microscopy [2], however, this conventional pick-and-place technique is time consuming for batch assembling of CNT based devices. Past demonstrations by K. Yamamoto et al. showed that carbon nanotube can be manipulated by AC and DC electric field [3, 4]. Besides, a recent report from L.A. Nagahara et al. demonstrated the individual single-walled carbon nanotube manipulation on nano-electrodes by AC bias voltage [5]. By using a similar technique, we have efficiently manipulated bulk MWNT to form resistive elements between Au microelectrodes for sensing application.

In this paper, we will present the technique to assembly bulk MWNT across microelectrodes using AC electrophoresis. Moreover, we will report our experimental findings on the dynamic characterization on these MWNT bundles such as frequency response, I-

V characteristics and TCR of the bulk MWNT devices. In the end, we will present the fabrication process of polymer-based MWNT embedded sensors which may potentially serve as micro/nano resolution sensors for various sensing applications.

AC ELECTROPHORETIC MANIPULATION OF MWNT BUNDLES

Theoretical Background

AC electrophoresis (or dielectrophoresis) is a phenomenon where neutral particles undergo mechanical motion inside a non-uniform AC electric field (see Fig. 1). Detailed descriptions on AC electrophoresis can be found in [6]. The dielectrophoretic force imparted on the particle can be described by the following equation:

$$\vec{F}_{DEP} = \frac{1}{2}\vec{\alpha}V\nabla\left|\vec{E}\right|^2 \quad (1)$$

where $\vec{\alpha}$ is the polarizability vector, which is a frequency dependent term. V is the volume of the particles and $\nabla = \vec{i}\frac{\partial}{\partial x} + \vec{j}\frac{\partial}{\partial y} + \vec{k}\frac{\partial}{\partial z}$ is the gradient operator. $\left|\vec{E}\right|$ is the magnitude of the electric field strength. From Equation (1), the direction of dielectrophoretic force is dependent on the electric field gradient rather than the sign of direction of the electric field. Besides, the polarizability vector also determines the direction of the forces (i.e. either repulsive or attractive). In physical sense, the dielectric particle undergoes polarization inside the electric field and attractive forces will be induced in different parts of the particle. If the electric field is non-homogenous, then the pulling forces acting on one side of the particle will be greater than the other side, which results a net force acting on the particle (see Fig. 2).

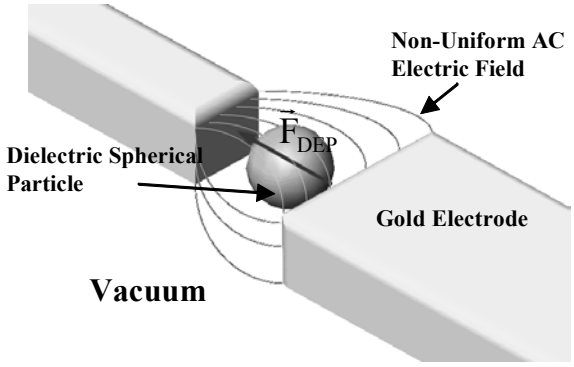

Fig 1. Principle of AC electrophoresis.

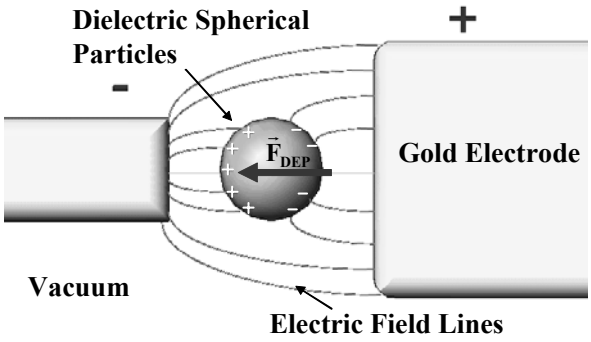

Fig 2. At a particular time instant, the dielectric particle undergoes polarization and non-zero net force will be induced inside non-homogenous electric field.

Experimental Process Flow for MWNT Bundles Formation

In order to manipulate bulk MWNT by AC electrophoresis, microelectrodes have to be fabricated on either glass substrate or silicon substrate. After the microelectrodes are fabricated, then the microelectrodes are wire-bonded to the external interfacing circuitry for external voltage excitation. Afterwards, the MWNT are then transferred to the substrate through the ethanol medium. The experimental process flow is shown in Fig. 3. Detailed explanations for each procedure will be given as follow.

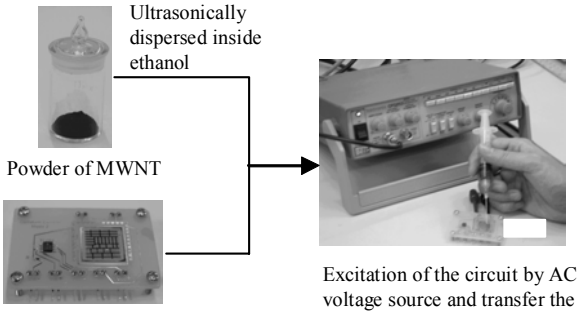

Figure 3. Experimental process flow showing the assembly of bulk MWNT across the microfabricated electrodes.

Microelectrodes Fabrication

In our experiments, arrays of Au microelectrodes (see Fig. 4) were fabricated on 1.8 X 1.8 cm^2 glass substrate and silicon substrate using either wet etching technique or lift-off technique. From our experimental observations, patterns with minimum feature size over 5 μm can be fabricated with smoother edges using lift off

technique whereas wet etching technique works well for feature size less than 5 μm at the expense of non-smooth edges. Detailed parameters for the procedures have been reported previously in [7].

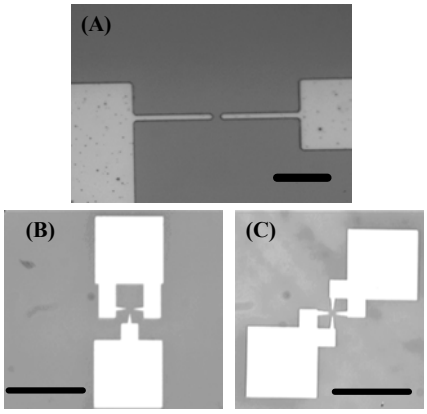

Fig 4. Optical microscopic images showing different designs of microelectrodes for MWNT manipulations. (A)Simple rectangular microelectrodes (Scale Bar = 30 μm). (B) T-microelectrodes to form V-shape MWNT geometry. (C) Cross microelectrodes to from parallel bundled MWNT geometry. (Scale Bar = 200 μm for (B) and (C)).

Sample Preparation for MWNT

MWNT used in our experiments were ordered commercially from [8]. According to the specifications from the manufacturer, these MWNT were prepared by chemical vapour deposition and their length and diameter were 1-10 μm and 10-30 nm, respectively. In our laboratory, 50 mg of MWNT was dispersed ultrasonically in 500 mL ethanol (absolute) for 30 minutes. The purpose of sonication is to disperse the MWNT individually throughout the ethanol medium to minimize the degree of aggregation. The resulting solution was then diluted to different concentrations (e.g. 0.01 mg/mL) for later experimental purposes.

Experimental Results for AC Electrophoretic Manipulations on MWNT

After the microelectrodes were fabricated and the MWNT were suspended inside ethanol medium, then the microelectrodes were wire-bonded to the external interfacing circuit as shown in Fig. 5. Afterwards, approximately 10 μL of dispersed MWNT suspension were transferred to the substrate by a 6 mL gas syringe. AC bias voltage was then applied across microelectrodes (16 V peak-to-peak and 1 MHz typically). The ethanol was then evaporated away leaving the MWNT between the gap of the microelectrodes. The formation of MWNT linkages could be confirmed by the scanning electron microscopic (SEM) image (See Fig. 6). By different design of microelectrode geometries (See Fig. 4 B and C), it is possible to manipulate MWNT bundles into different directions (See Fig. 7).

It was experimentally found that the room temperature resistances of MWNT bundles were sample dependent (i.e. different MWNT samples had different room temperature resistances) and the two probe room temperature resistances of the samples were typically ranged from several kΩ and several hundred kΩ.

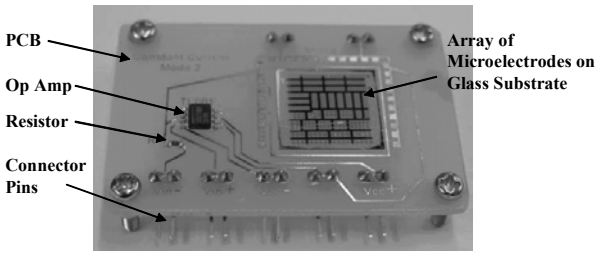

Fig 5. CC mode circuitry acts as interfacing circuit..

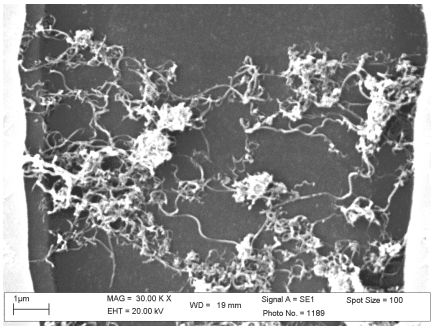

Fig 6. SEM image showing the formation of MWNT linkages between the microelectrodes.

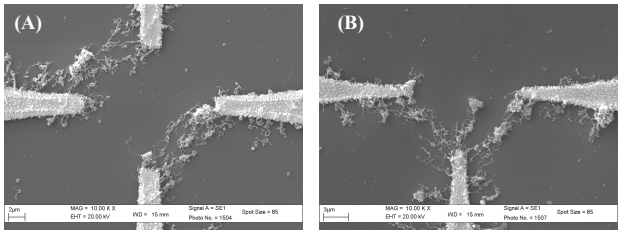

Fig 7. SEM images showing special alignment of MWNT bundles. A) MWNT bundles were aligned in parallel directions by the cross microelectrodes. B) MWNT bundles were aligned into V-shape by the T microelectrodes.

CNT AS THERMAL SENSING ELEMENT FOR MICRO ANEMOMETRY

Thermal Sensitivity

Bundled MWNT was used as thermal sensing element driven in CC mode configuration (see Fig. 8). In order to measure the temperature-resistance relationship of the bundled MWNT device, the hybrid

integrated circuit was put inside an oven (Lab-Line® L-C Oven) and the temperature of the environment was kept monitored by Fluke type K thermocouples attached on the surface of the circuit board. The TCR was then obtained by measuring the change of resistance of the bundled MWNT with the corresponding temperature. From the experimental measurements on a typical bundled MWNT device, its resistance dropped with temperature, which is in agreement with [9] (i.e. negative TCR). Interestingly, the TCR measurements of all of our testing devices did not converge but the ranges were generally within -0.1 to -0.2 %/°C . Considerable drifting in room temperature resistances of the device were observed in different measurements (See Fig. 9). We suspect the variations were contributed by the mismatch in thermal coefficient of expansion between Au microelectrodes and the bundled MWNT, causing some of the MWNT linkages detach from the Au microelectrodes. Another possible reason could be the effect of contaminations such as moisture during measurements. In order to form a more robust protection for MWNT bundles, we are currently developing a process to embed MWNT bundles between parylene layers to see its effectiveness. The details of the fabrication process will be explained in later section. Nevertheless, the temperature-resistance dependency of bundled MWNT implied its thermal sensing capability.

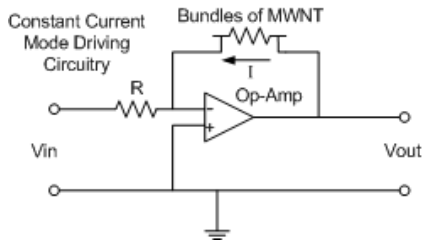

Fig. 8. Schematic diagram showing the typical CC mode configuration in the experiments.

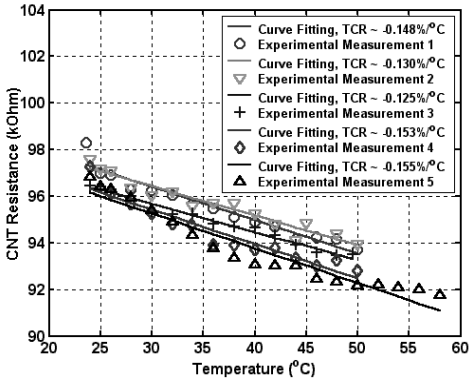

Fig. 9. TCR for a typical bundled MWNT device in five different measurements.

Frequency Response

In order to pick up fast time-varying parameters in a sensed environment, sensors with fast frequency response are highly desired. To test the frequency response of the bundled MWNT device, input square wave of 2 V peak-to-peak at 10 kHz was fed into the negative input terminal of the circuit as shown in Fig. 8 and the output response was determined (see Fig. 10). From our experimental measurements, bundled MWNT device exhibited very fast frequency response. Using the approximation between the time constant and cutoff frequency [10],

$$\mathbf{f_c} = 1/(1.5 \cdot \mathbf{t_c}) \qquad (2)$$

where f_c is the cutoff frequency, t_c is the time constant of the response, and therefore the estimated cutoff frequency of the device was about 177 kHz (see Fig. 10). As a comparison, typical frequency response of MEMS polysilicon sensors in CC mode configuration without frequency compensation is around several hundred Hz to several kHz [10, 11].

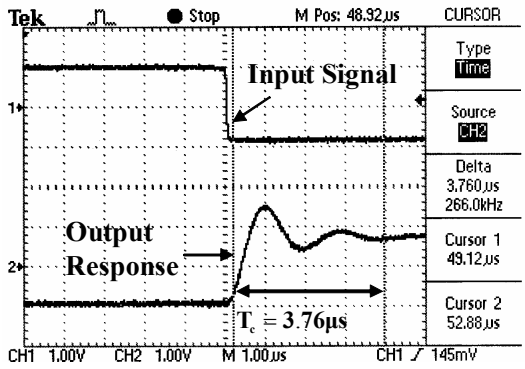

Fig. 10. Frequency response of MWNT bundles in CC mode configuration.

Power Consumption

From the I-V characteristics of the MWNT bundles, the current required to induce the self heating of the elements was in μA range at several volts which suggested that the power consumption of the device was in μW range. For example, in our sample circuit, only 3.6 μA at 0.6 V was required to induce self heating of the MWNT bundles (See Fig. 11).

A proof-of-concept experiment was performed to validate the flow sensing ability of MWNT bundles in μW operating power. The CNT sensor was placed perpendicular to a flow source with constant outlet velocity (see Fig. 12). The distance between the source and the sensor was then varied to induce different impinging velocities on the sensor (similar to Hiemenz flow). Although the flow environment was not well-controlled, results do clearly indicate the response of the sensor to different impinging velocities (see Fig. 13).

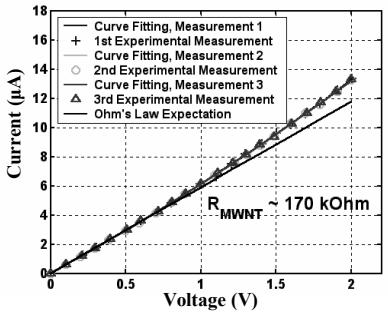

Fig. 11. Typical I-V characteristics of the MWNT bundles. Three repeated measurements were performed to validate the repeatability. Experimental measurements were fitted into second order curves by least square method. The straight line is the theoretical expectation by Ohm's Law and the room temperature resistance of the MWNT bundles in the testing sample is about 170 kOhm.

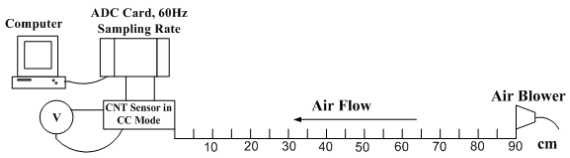

Fig. 12. Schematic diagram showing the experimental setup for simple air blowing testing. The CNT sensor was placed in normal to the direction of the air flow.

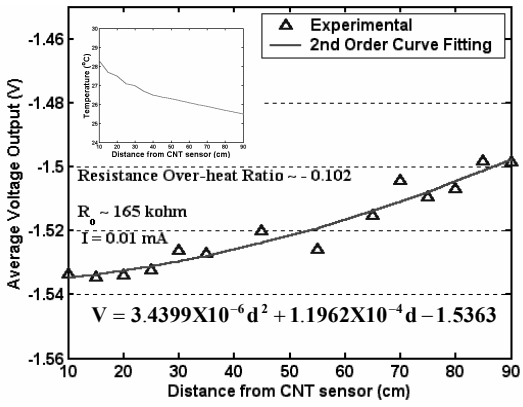

Fig. 13. Output voltage variations with the air flow at different locations between the sensor and the air blower. Inset shows the temperature of the air flow at different locations and the range was generally within 2 °C. The operating power of the sensor was about 15 μW.

FABRICATION OF PARYLENE/CNT/PARYLENE EMBEDDED SENSORS FOR MICRO/NANO FLUIDIC APPLICATIONS

Owing to the ultra low power consumption (~ μW) of CNT based sensors, CNT can sense the surrounding physical parameters (such as temperature or fluid motion) with minimal thermal disturbances to the environment. Therefore, CNT is very promising to sense physical parameters in micro scale or even nano scale world where the true parameters are easily overwhelmed by thermal disturbances.

Currently, we are fabricating three versions of MWNT based sensors for the investigations of their thermal sensing properties. For the first version (see Fig. 14), the MWNT bundles rest between the Au microelectrodes without parylene C coating which is presented in the previous sections. For the second version (See Fig. 15), the MWNT bundles rest on a parylene C layer and connected across the Au microelectrodes. For the third version (see Fig. 16), the MWNT bundles are embedded inside parylene C layers.

The general fabrication process for version III of the MWNT sensor is shown in Fig. 17. To start with, a glass substrate was first patterned with Au microelectrodes with Cr or Ni as interfacing layer for better adhesion with the substrate [7]. Then, the parylene C layer was deposited on the substrate using parylene deposition machine (PDS 2010 LABCOATER® 2) and then patterned to the desired geometry inside oxygen plasma. This parylene layer serves as a bottom layer to isolate the bundled MWNT from the substrate. In order to form the MWNT bundles more effectively across the microelectrodes, the step size of this parylene bottom layer should be smaller than that of the Au microelectrodes. Afterwards, MWNT was then transferred to the substrate and form across the microelectrodes by AC electrophoresis as mentioned in the previous section. Finally, parylene C layer were deposited on the substrate and then patterned to the desired geometry. This layer served as the top layer to embed the MWNT bundles completely inside the parylene C layers. For Version II MWNT sensor, this final procedure was omitted.

CONCLUSION

A technique to form bundled MWNT across Au microelectrodes using AC electrophoresis was presented. By using special microelectrode geometries, it is possible to manipulate the MWNT bundles into different alignments.

Besides, preliminary characterization of the version I MWNT sensor such as the frequency response, thermal sensing capability and the power consumption was presented. Since the sensors are capable to operate at μW power range, they are very promising to be used for high performance micro/nano resolution sensing for micro/nano fluidic applications.

Finally, we have presented the fabrication process of the version II and version III MWNT sensors and we are currently characterizing the mechanical and thermal properties of them. Wind tunnel tests for all versions of MWNT sensors will be carried out later. Detailed

analysis for different versions of MWNT sensors will be published else where at a later time.

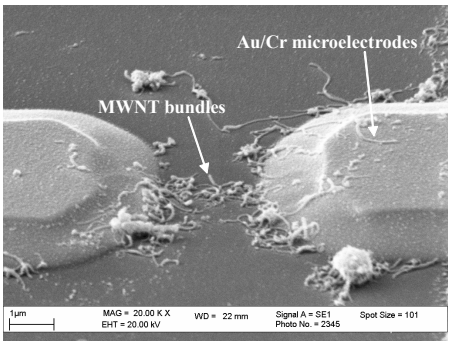

Fig. 14. SEM image showing the version I of the MWNT bundled sensor. The MWNT bundles are connected across the microelectrodes and rest on the glass substrate.

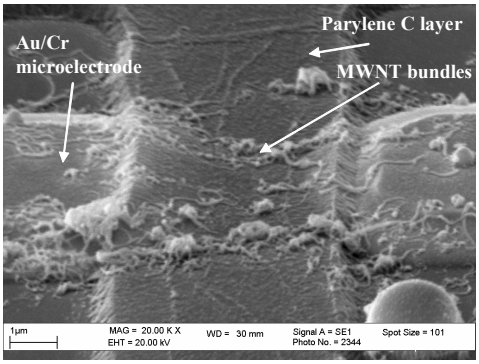

Fig. 15. SEM image showing the version II of MWNT bundled sensor. The MWNT bundles are connected across the microelectrodes and rest on the parylene C layer.

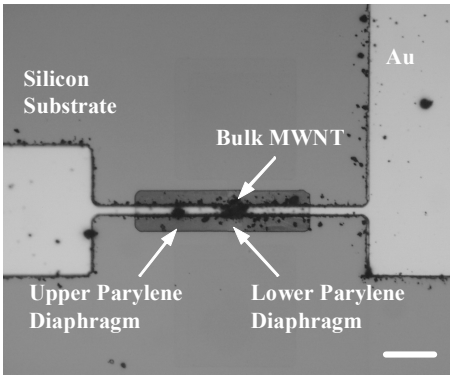

Fig. 16. Optical microscopic image showing the version III of the MWNT bundled sensor. The MWNT bundles are embedded inside the parylene C layers. Since embedded MWNT bundles cannot be visualized clearly by SEM image, optical microscopic image is used instead. (Scale Bar = 20 µm.)

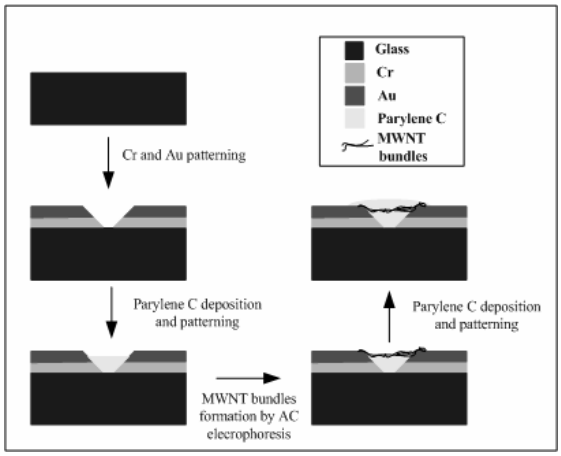

Fig. 17. Fabrication process flow for the version III MWNT sensor.

REFERENCES

[1] J.B. Huang, C. Liu, F. Jiang, S. Tung, Y.C. Tai, C.M. Ho, "Fluidic Shear Stress Measurement Using Surface-Micromachined Sensors", Proceedings of IEEE Region 10 International Conference on Microelectronics and VLSI 1995, pp. 16 – 19 (1995).

[2] T. Shiokawa, K. Tsukagoshi, K. Ishibashi, Y. Aoyagi, "Nanostructure Construction in Single-walled Carbon Nanotubes by AFM Manipulation", Proceedings of Microprocesses and Nanotechnology Conference 2001, pp. 164 – 165 (2001).

[3] K. Yamamoto, S. Akita, Y. Nakayama, "Orientation of Carbon Nanotubes Using Electrophoresis", Japanese Journal of Applied Physics, Vol. 35, L917 – L918 (1996).

[4] K. Yamamoto, S. Akita, Y. Nakayama, "Orientation and Purification of Carbon Nanotubes Using AC Electrophoresis", Journal of Physics D: Applied Physics, Vol. 31, L34 – L36 (1998).

[5] L.A. Nagahara, I. Amlani, J. Lewenstein and R.K. Tsui, "Directed Placement of Suspended Carbon Nanotubes for Nanometer-scale Assembly", Applied Physics Letters, Vol. 80, No. 20, pp. 3826 – 3828 (2002).

[6] H.A. Pohl, "Dielectrophoresis: The Behaviour of Neutral Matter in Nonuniform Electric Fields", Cambridge University Press (1978).

[7] V.T.S. Wong, Wen J. Li, "Dependence of AC Electrophoresis Carbon Nanotube Manipulation on Microelectrode Geometry", International Journal of Non-linear Sciences and Numerical Simulations, Vol. 3, Nos. 3 -4, pp. 769 – 774 (2002).

[8] Sun Nanotech Co Ltd, Beijing, P.R. China.

[9] T.W. Ebbesen, H.J. Lezec, H. Hiura, J.W. Bennett, H.F. Ghaemi, T. Thio, "Electrical Conductivity of Individual Carbon Nanotubes", Nature, Vol. 382, pp. 54 – 56 (1996).

[10] C. Liu, J.B. Huang, Z. Zhu, F. Jiang, S. Tung, Y.C. Tai, C.M. Ho, "A Micromachined Flow Shear-Stress Sensor based on Thermal Transfer Principle", Journal of Microelectromechanical Systems, Vol. 8, No. 1, pp. 90 – 99 (1999).

[11] J.B. Huang, F.K. Jiang, Y.C. Tai, C.M. Ho, "MEMS-based Thermal Shear-stress Sensor with Self-frequency Compensation", Measurement Science and Technology, Vol. 10, No. 8, pp. 687 – 696 (1999).